Exploring the aqueous photodegradation of three ionizable macrolide antibiotics: Kinetics, intermediates and photoinduced toxicity

Linke Ge[a,b,1], Nannan Cui[a,1], Yan Yang[a], Crispin Halsall[b], Shengkai Cao[a,b], Peng Zhang[a,*]

[a]School of Environmental Science and Engineering, Shaanxi University of Science & Technology, Xi'an 710021, P. R. China

[b]Lancaster Environment Centre, Lancaster University, Lancaster LA1 4YQ, United Kingdom

[1]These authors contributed equally to this work.

Abstract:

Three macrolide antibiotics (MLs, e.g., roxithromycin, clarithromycin and spiramycin) were investigated to reveal the aqueous photochemistry of the respective neutral and dissociated species i.e. H_2MLs^+, $HMLs^0$ and MLs^-. including their susceptibility to direct photolysis as well as the hydroxyl radical (•OH) and singlet oxygen ($^1O_2$) mediated photooxidation. Under simulated sunlight (λ > 290 nm), no obvious loss or slow photodegradation of the three MLs were observed in pure water althoughthey photodegraded rapidly under shorter wavelength irradiation (λ > 200 nm). It was further found that the dependence of the kinetics on pH was attributed to the different reactivities of the dissociation species. The rate constants and cumulative light absorption increased from H_2MLs^+ > $HMLs^0$ > MLs^-. Based on competition kinetic experiments and matrix calculations, MLs^- was differentiated to be more highly reactive towards •OH/$^1O_2$. The corresponding environmental half-lives were evaluated considering the reactivities and proportions of the speciated forms at different pH, indicating that $^1O_2$ oxidation ($t_{1O2,E}$ = 1.83 – 2.53 h) contributed more than •OH oxidation ($t_{•OH,E}$ = 33.17 – 787.49 h) to the ML phototransformation in sunlit surface waters (pH = 6 – 9). In general these reactions

* Corresponding author.

E-mail address: zhangpeng4477@sust.edu.cn (P. Zhang).

preserved the core backbone structures of the parent ML molecules and gave rise to intermediates (photolytic byproducts identified using HPLC-MS/MS) that displayed higher toxicity than the parent molecules (luminescence inhibition test of *Vibrio fischeri*) hence demonstrating photo-modified toxicity. These results are of importance towards the goal of assessing the persistence of ML during wastewater treatment using UV-light tertiary treatment processes, as well as in sunlit surface waters and.

Keywords: Macrolide antibiotics; Dissociation species; Photodegradation kinetics; Transformation pathways; Photomodified toxicity

1. Introduction

There are many ionisable or dissociable organic micropollutants in environmental waters, such as pharmaceuticals like macrolide, fluoroquinolone and sulfonamide antibiotics, as well as hydroxylated polybrominated diphenyl ethers, tetrabromobisphenol A, triclosan etc. Their molecular structures contain ionizable groups such as carboxyl (-COOH), hydroxyl (-OH) and/or amino (-NH_n) groups, ensuring their presence in aquatic systems will be as their neutral and/or dissociated forms depending on the ambient pH Many previous studies have shown that the dissociated forms of organic pollutants have unique physicochemical properties that differ from the neutral form of the molecule (e.g., aqueous solubility, octanol-water partition coefficient, etc.), and exhibit different environmental behavior as a consequence (Wei et al. 2013, Xie et al. 2013) (Ge et al. 2019) as well differing toxicity (Yang et al. 2013) In the aqueous euphotic zone, photochemical transformation is an important pathway for many organic pollutants. These pollutants can directly absorb sunlight and undergo apparent photolysis, including direct photolysis and self-sensitized photodegradation. Importantly, chemical pollutants are likely to undergo indirect photodegradation or sensitized photooxidation mediated by photochemically active substances in excited states such as reactive oxygen species (ROS, including •OH and $^1O_2$) (Cooper et al. 1989, Ge et al. 2016, Niu et al. 2013) (Ge

et al. 2018b). In comparation with non-dissociable compounds, dissociable organic pollutants exhibit more complex photochemical behavior, as the various dissociated forms may exhibit different susceptibilities to phototransformation In the process, not only different photochemical reactions of each single dissociated form should be considered, but also the multivariate phototransformation half-lives of all dissociated forms need to integrated in order to assess the environmental photochemical fate of ionisable pollutants. In view of this, it is necessary to select representative dissociable compounds to reveal their complex photochemical transformation kinetics, intermediates in order to understand their environmental fate.

Antibiotics are increasingly detected as aqueous contaminants, and exist as different dissociated species depending on the pH of the water. Their decay in sunlit surface waters is governed to a large extent by photochemical transformation. The photochemical behavior of different dissociated species of the same compoundhas been studied for specific classes of antibiotics, such as fluoroquinolones (FQs) (Ge et al. 2015, Wei et al. 2013) (Ge et al. 2018b), sulfonamides (SAs) (Boreen et al. 2004, 2005, Willach et al. 2018) (Ge et al. 2019) and tetracyclines (TCs) (Niu et al. 2013, Werner et al. 2006) (Ge et al. 2018a). In the previous studies, individual classes of antibiotics showed different photochemical reaction kinetics or reactivities of the various dissociated forms. For example, neutral FQs ($HFQs^0$) photodegraded the fastest, followed by fully protonated (H_2FQs^+), and anionic forms (FQs^-) (Ge et al. 2015), whereas TCs^{2-} was found to be the most highly reactive towards apparent photolysis among the three dissociated forms of TCs (Ge et al. 2018a). As for the •OH mediated photooxidation, $HFQs^0$ reacted the fastest with •OH (Ge et al. 2015), while SAs^- were more reactive towards •OH than $HSAs^0$ and H_2SAs^+ for the majority of the SAs (Ge et al. 2019). Given this different behavior, the photochemistry of different dissociated species is interesting and their reaction kinetic patterns are dependent on the classes of antibiotics. Thus, the aqueous photochemistry needs to

73 be investigated further for other classes of antibiotics in different dissociation forms, as it likely
74 affects their fate and longevity in surface waters associated with pH changing from 6 to 9
75 (Schwarzenbach et al. 2003).

76 Among the antibiotics commonly detected in surface waters, macrolides (MLs) are
77 ubiquitous as aquatic contaminants, and capable of existing as different dissociated formsforms
78 within the pH range of 6 – 9. Compared with FQs, SAs and TCs (Zhang et al. 2019) (Geng et
79 al. 2020) (Garcia-Galan et al. 2012) (Ge et al. 2019) (Ge et al. 2018a) (Li et al. 2018), the
80 photochemistry of MLs is not well understood , which may be attributed to their more complex
81 chemical structure, containing 12-16 carbon lactone rings and many ionizable groups. Only a
82 few MLs such as tylosin and azithromycin have been studied with regards to their
83 photochemical kinetics and intermediates (Voigt and Jaeger 2017). In previous related studies,
84 the effect of pH on the apparent photolysis and ROS oxidation of MLs were examined,
85 indicating that the reaction rate constants were dependent on pH (Voigt and Jaeger 2017) (LV
86 et al. 2019) (Li et al. 2019). These studies clarified the pH dependence of ML
87 phototransformation, although the distinct kinetics were not determined for the various
88 dissociated species of each ML.

89 In the present study, we selected roxithromycin (ROX), spiramycin (SPI) and clarithromycin
90 (CLA) as model compounds and investigated their multivariate photochemical behavior:
91 apparent photolysis, and ROS (•OH and $^1O_2$) photooxidation of the various dissociated forms.
92 As for the MLs, they are increasingly detected in aquatic environments in many industrialized
93 regions, including countries like China where antibiotic use is extensive (Fig. S1). ROX, SPI
94 and CLA have been observed as ubiquitous MLs in surface waters with reported mean
95 concentrations of 56 ng L^{-1}, 16 ng L^{-1} and 52 ng L^{-1}, respectively (Li et al. 2022). These
96 compounds are ionizable, and may exhibit three dominant dissociated forms in water (Fig. S2).
97 In the study, the oxidation kinetics and reactivities were examined for the three dissociated

forms with important implications for how we assess their fate as well as undertake environmental risk assessments for this group of chemicals.

2. Materials and methods

2.1. Reagents and materials

Three MLs (ROX, SPI, and CLA) were obtained from different suppliers with > 98% purity (Table S1). Sodium acetate, ammonium acetate and formic acid were of HPLC grade and purchased from Shanghai Macklin Biochemical Technology Co., Ltd. Acetophenone (AP, purity > 98.5%) was provided by TCI Development Co., Ltd (Shanghai, China). Perinaphthenone (97% purity) was obtained from Sigma-Aldrich. Information of other chemicals used are shown in Table S1. All solutions were prepared in ultrapure water obtained from a Millipore-Milli Q system.

2.2. Apparent photolysis experiments

All photochemical experiments were carried out in a merry-go-round photochemical reactor, and the experimental setup is illustrated in Fig. S3. In the apparent photolysis experiments, a quartz-filtered and water-refrigerated 500 W high-pressure mercury lamp was used as UV-Vis light source (λ > 200 nm). When simulated sunlight (λ > 290 nm) was needed, the lamp was fitted with with a Pyrex filter. Emission spectra of the light sources were measured by an Acton SP-300 monochromator, and the absorption spectra of the model compounds were determined by a TU-1901 double-beam UV-Vis spectrophotometer.

In order to investigate the apparent photolytic kinetics of MLs in different pH solutions, each of the ML antibiotics was dissolved in pure water with the initial concentration (C_0) of 10 μM (i.e well within their limits of aqueous solubility)and the solution pH adjusted to the desired

values with HCl/NaOH. Reaction solutions were added into quartz tubes (20 mm diameter and 50 mL volume), put in the reactor and irradiated with the suitable light. Samples were taken at regular intervals and the residual concentrations were analyzed by HPLC. The quantum yields (Φ) of MLs under UV-Vis (λ > 200 nm) irradiation were determined using potassium ferrioxalate as a chemical actinometer, detailed in the supplementary material.

2.3. Photoinduced ROS oxidation experiments

To explore the photoinduced ROS oxidation reactivities of MLs, competition kinetics were employed to determine the bimolecular rate constants ($k_{\bullet OH,MLs}$ and $k_{^1O2,MLs}$) of MLs with •OH/$^1O_2$ in pure water and at pH = 8, 10 and 12. For the •OH photooxidation experiments, H_2O_2 and AP (10 μM) were utilized as the •OH photosensitizer and reference compound, respectively, with the irradiation of simulated sunlight (λ > 290 nm). In order to ensure the steady-state concentration of •OH and the appropriate sampling intervals, 100 mM and 20 mM H_2O_2 was used in the ROX, CLA reaction systems and in the SPI system, respectively. Under simulated solar irradiation, MLs might undergo apparent photolysis (Fig. S4), so it is necessary to correct the apparent photolytic rate constants (k_P) according to Eq. 1, and then to calculate the bimolecular reaction rate constants ($k_{\bullet OH,MLs}$) according to Eq. 2.

$$k_p = \frac{\sum I_\lambda T_\lambda \dfrac{\varepsilon_\lambda [\mathrm{MLs}]}{\varepsilon_\lambda [\mathrm{MLs}] + \varepsilon_{\lambda,H_2O_2} [H_2O_2]}}{\sum I_\lambda T_\lambda \varepsilon_\lambda} k' = f k' \quad (1)$$

$$k_{\bullet OH,MLs} = \frac{\left(k_{CKE} - k_p\right) k_{\bullet OH,AP}}{k_{CKE,AP}} \quad (2)$$

where f is a weighting factor considering the light attenuation of H_2O_2; k' is the apparent photolysis rate constants of MLs without H_2O_2; k_{CKE} and $k_{CKE,AP}$ represent the apparent

degradation rate constants of MLs and AP in competitive kinetic experiments, respectively. I_λ represents the relative light intensity of the irradiation light (Fig. S4), and T_λ is the transmittance of the Pyrex well; ε_λ and $\varepsilon_{\lambda,H2O2}$ are the molar absorptivities of MLs and H_2O_2, respectively. $k_{\bullet OH,AP}$ is equal to 5.9×10^9 M^{-1} s^{-1}, representing the bimolecular reaction rate constants of AP with •OH (Edhlund et al. 2006) (Ge et al. 2016).

For the $^1O_2$ photooxidation experiment, 420 nm cut-off filters were used to obtain the appropriate light irradiation (Fig. S3). Perinaphthenone (20 μM) and FFA (10 μM) were utilized as the $^1O_2$ photosensitizer and reference compound ($k_{1O2,FFA}$=1.2×10^8 M^{-1} s^{-1}), respectively. The corresponding calculation equation referred to our previous studies (Ge et al. 2015) (Ge et al. 2019). All the irradiation experiments with controls were carried out in triplicate.

2.4. Analysis determination

An Agilent 1260 HPLC fitted with ZORBAX Eclipse Plus C18 column (3.0 mm × 150 mm, 1.8 μm) and Variable Wavelength Detector (VWD), was employed for the separation and quantification of MLs, AP and FFA in the irradiated samples. The mobile phase was ammonium acetate solution (10 mM) and acetonitrile. Photolytic products were analyzed by an Agilent 6470B HPLC-MS/MS equipped with an electrospray ionization (ESI) source. These instrumental conditions and parameters are detailed in the supplementary material (Table S2).

2.5 Bioassay

The bioluminescence inhibition assay using *Vibrio fischeri* was adopted to examine the photomodified toxicity during the MLs degradation. The 15 min acute ecotoxicity was carried out following the international standard method (ISO11348-3-2007), and USA HACH Eclox

water-quality detector was used to record luminous intensities. Luminescence inhibition rates (I%) were calculated according to Eq. 3,

$$I\% = \frac{(I_0 - I_{15})}{I_0} \times 100\% \quad (3)$$

where I_0 represents the intensity of the sample at 0 min, and I_{15} is the luminous intensity of the sample after 15 min.

3. Results and discussion

3.1. Apparent photolytic kinetics and quantum yields

As for dark controls, no obvious loss (degradation ratio < 3%) of the three MLs in pure water were observed. When exposed to simulated solar irradiation (λ > 290 nm) for 4 h (Fig. 1), CLA and SPI experienced substantial photodegradation (> 31% and 1.5%, respectively), while negligible degradation (< 0.3%) was observed for ROX. This can be attributed to the absorption spectra of MLs (Fig. S4), in which CLA and SPI exhibit weak light absorption at λ > 290 nm whereas as ROX showed negligible absorption. Batchu et al (Batchu et al. 2014) also found that ROX was persistent in pure water under simulated sunlight. Furthermore, the photolytic data of CLA and SPI exhibited exponential decay (R^2 > 0.98), indicating that the photoreaction followed pseudo-first-order kinetics (Fig. 1). The corresponding apparent photolytic rate constants (k_P) were calculated to be 0.0088 ± 0.0003 min^{-1} and 0.0005 ± 0.0001 min^{-1}, respectively. In comparison with tetracyclines ($t_{1/2}$ = 0.01 h – 5.37 h) under a similar irradiation regime (Ge et al. 2018a), the half-lives ($t_{1/2}$ = 1.31 h – 23.11 h) of the MLs were larger, indicating their solar apparent photodegradation in surface waters would be very slow.

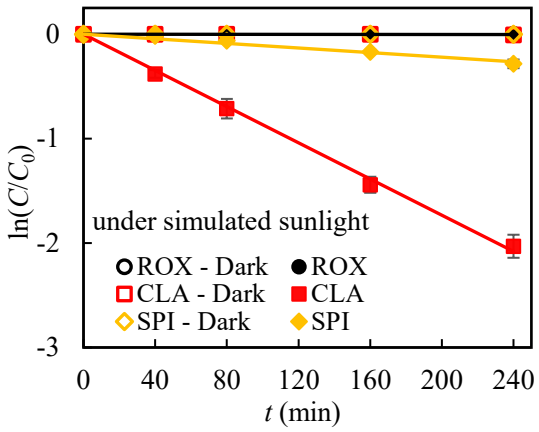

Fig. 1. Apparent photolysis kinetics of the three MLs in pure water and under simulated sunlight (λ > 290 nm)

In view of the slow photodegradation of MLs under simulated sunlight, their photolysis in pure water under UV-Vis irradiation (λ > 200 nm) were further investigated (Fig. 2). UV−Vis irradiation is widely used for disinfection of aquatic systems and pollution remediation in wastewater (Khajouei et al. 2022). The three MLs were found to degrade quickly due to their significant light absorption from 200 nm to 290 nm (Fig. S4), with the k_p ranging from 0.0216 ± 0.0010 min^{-1} for ROX to 0.0883 ± 0.0009 min^{-1} for SPX in pure water. Furthermore, the apparent photolytic kinetics of MLs were explored as a function of different pH values (Fig. 2). The k_p values were found to be elevated with increasing pH, which might be attributed to the diverse distribution of the dissociation forms (H_2MLs^+, $HMLs^0$ and MLs^-) at different pH (Table S3), as well as the different photochemical reactivities of the various chemical forms.

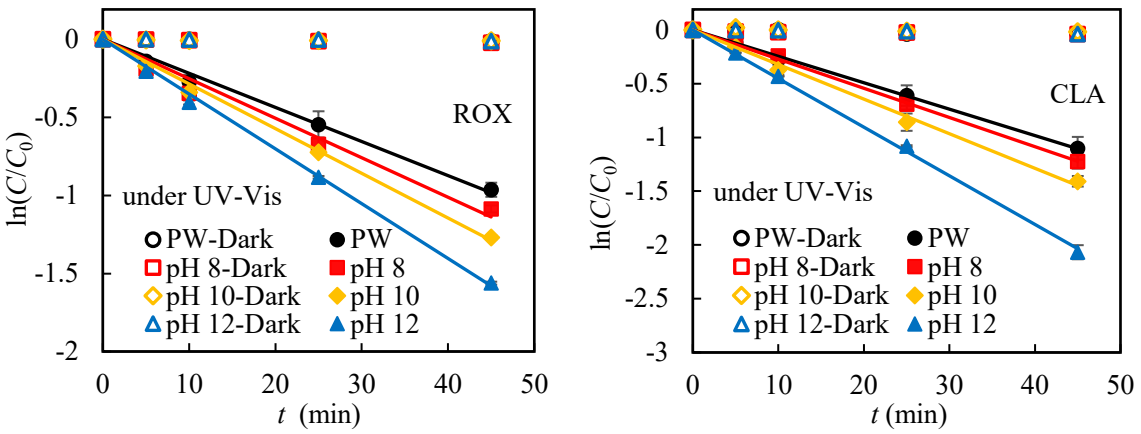

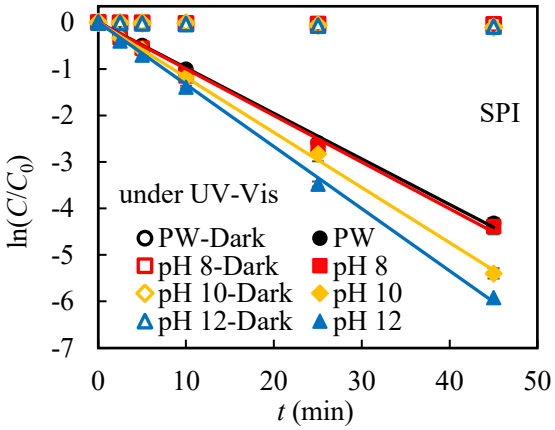

Fig. 2. Apparent UV-Vis photolytic kinetics of MLs in pure water (PW) and different pH solutions

Based on matrix calculations in our previous study (Ge et al. 2018b), the apparent photolytic rate constants ($k_{p,i}$) and quantum yields (Φ_i) can be obtained for the different ML dissociated forms (i). As shown as in Table 1, MLs^- photodegraded the fastest, followed by $HMLs^0$ and H_2MLs^+. As for SAs and TCs, their anionic forms also underwent the faster photodegradation (Ge et al. 2019) (Ge et al. 2018a). However, the photodegradation of neutral FQs was faster than other dissociation forms (Li et al. 2020) (Ge et al. 2018b). This demonstrated that the different classes of antibiotics showed diverse apparent photolytic reactivities. And even for one class of antibiotics, the different dissociation species had various $k_{p,i}$ and Φ_i, accounting for the dependence of apparent photolytic kinetics on pH.

Theoretically, k_p for organic pollutants in dilute aqueous solutions can be expressed as Eq. 4,

$$k_p = 2.303\Phi\sum L_\lambda\varepsilon_\lambda \quad (4)$$

where L_λ is the light irradiance, and ε_λ is the molar extinction coefficient (Fig. S5). Thus, the magnitude of k_p depends on the cumulative light absorption ($\Sigma L_\lambda\varepsilon_\lambda$) and Φ. As shown in Table 1, when the dissociation species changed from H_2MLs^+, $HMLs^0$ to MLs^-, the corresponding $k_{p,i}$ increased, whereas Φ_i decreased. Therefore, it is $\Sigma L_\lambda\varepsilon_\lambda$ for the different dissociation species that dominates their $k_{p,i}$ values.

Table 1. Apparent photolysis kinetic parameters and quantum yields (Φ_i) of different ML dissociation

species (i) under UV-Vis irradiation.

Antibiotics	Dissociation species (i)	$k_{p,i}$ (min^{-1})	$t_{1/2,i}$ (min)	Φ_i
roxithromycin (ROX)	H_2ROX^+	0.0216 ± 0.0012	32.13 ± 1.78	0.1877 ± 0.0104
	$HROX^0$	0.0275 ± 0.0003	25.25 ± 0.32	0.1446 ± 0.0018
	ROX^-	0.1033 ± 0.0058	6.72 ± 0.38	0.0351 ± 0.0020
clarithromycin (CLA)	H_2CLA^+	0.0271 ±0.0012	25.60 ± 1.09	0.1927 ± 0.0082
	$HCLA^0$	0.0304 ± 0.0013	22.83 ± 0.96	0.1589 ± 0.0067
	CLA^-	0.2180 ±0.0031	3.18 ± 0.05	0.0642 ± 0.0009
spiramycin (SPI)	H_2SPI^+	0.0837 ± 0.0043	7.99 ± 0.43	0.0163 ± 0.0008
	$HSPI^0$	0.1142 ± 0.0031	5.96 ± 0.17	0.0208 ± 0.0006
	SPI^-	0.3245 ± 0.0100	2.09 ± 0.07	0.0335 ± 0.0010

3.2 Photooxidation kinetics of dissociation forms

In the control experiments under irradiation of $\lambda > 290$ nm and in the absence of the •OH photosensitizer, the loss of individual MLs was > 15%, which indicated that apparent photolysis of MLs cannot be ignored, and should be corrected (Eq. 1). Whereas, the loss of MLs in the control experiments of $^1O_2$ oxidation ($\lambda > 420$ nm) was negligible (< 0.5%). The corrected $k_{\bullet OH,MLs}$ were obtained in pure water and at different pH values (Table S4), indicating that the $k_{\bullet OH,MLs}$ increased when the pH changed from 8 to 12. As for the photoreaction with $^1O_2$ in pure water, SPI degraded significantly ($k_{^1O2,SPI} = 3.26 \pm 0.19 \times 10^7$) rather than ROX and CLA (Fig. S6), suggesting that only SPI can be oxidized by $^1O_2$. This can be attributed to alkene and conjugated diene moieties involved in the molecular structure of SPI, which were readily oxidized by $^1O_2$ (Ge et al. 2022) (Larson and Weber 1996, Mill 1999). Furthermore, the bimolecular reaction between SPI and $^1O_2$ was also facilitated by increasing pH.

The bimolecular reaction rate constants ($k_{ROS,i}$, e.g., $k_{\bullet OH,i}$ and $k_{^1O2,i}$) were differentiated for each dissociated species (H_2MLs^+, $HMLs^0$ and MLs^-) according to matrix calculations (Eq. 5):

$$\overset{\text{pH 8}}{\underset{\text{pH 12}}{\begin{pmatrix} \delta_{H_2MLs^+}, & \delta_{HMLs^0}, & \delta_{MLs^-} \\ \vdots & & \vdots \\ \vdots & & \vdots \end{pmatrix}}} \begin{pmatrix} k_{ROS,H_2MLs^+} \\ k_{ROS,HMLs^0} \\ k_{ROS,MLs^-} \end{pmatrix} = \overset{\text{pH 8}}{\underset{\text{pH 12}}{\begin{pmatrix} k_{ROS,MLs} \\ \vdots \\ \vdots \end{pmatrix}}} \quad (5)$$

where δ_i represents the fraction of each dissociated form, and $k_{ROS,MLs}$ is $k_{\bullet OH,MLs}$ or $k_{^1O2,MLs}$ at different pH. As shown in Table 2, both the $k_{\bullet OH,i}$ and $k_{^1O2,i}$ increased from H_2MLs^+, $HMLs^0$ to MLs^-, and the anionic MLs were the most reactive toward •OH and $^1O_2$. As for SPI, the $k_{\bullet OH,i}$ values of were 1 – 2 orders of magnitude larger than $k_{^1O2,i}$, indictive of the higher reactivity of •OH. Similar to the MLs, TCs and the majority of SAs in the anionic form were more reactive towards •OH and $^1O_2$ (Ge et al. 2018a) (Ge et al. 2019). However, neutral FQs showed higher reactivities toward •OH than the cationic and anionic forms (Ge et al. 2018b).

Furthermore, the environmental half-lives ($t_{ROS,E}$, e.g., $t_{\bullet OH,E}$ and $t_{^1O2,E}$) for MLs reacting with •OH and $^1O_2$ at specific pH in the euphotic zone of sunlit surface waters were calculated referring to Eqs. 6 and 7:

$$k_{ROS,E} = [ROS]\sum(\delta_i k_{ROS,i}) \quad (6)$$

$$t_{ROS,E} = \frac{\ln 2}{k_{ROS,E}} \quad (7)$$

where $k_{ROS,E}$ is the environmental rate constant of SAs towards •OH or $^1O_2$; $k_{ROS,i}$ represents $k_{\bullet OH,i}$ or $k_{^1O2,i}$; and [ROS] represents the environmental levels of 10^{-15} M for •OH and 10^{-12} M for $^1O_2$, respectively (Cooper et al. 1989, Mill 1999) (Xu et al. 2011) (al Housari et al. 2010). As illustrated in the Table 2, in the conditions of most fresh and sea waters (pH = 6 – 9), $t_{\bullet OH,E}$ ranged from 33.17 h for SPI to 787.49 h for CLA, while $t_{^1O2,E}$ of SPI ranged from 1.83 h to 2.53 h. This indicated that photo-induced $^1O_2$ oxidation contributed more to the phototransformation of the ML antibiotics compared with their •OH oxidation in sunlit surface waters. Similarly, $^1O_2$ oxidation plays a key role for the aqueous environmental

phototransformation of SAs (Ge et al. 2019).

Table 2. The bimolecular reaction rate constants ($k_{\bullet OH,MLs}$ and $k_{^1O2,MLs}$)of the different dissociated MLs with $\bullet OH/^1O_2$, and the corresponding environmental half-lives ($t_{\bullet OH,E}$ and $t_{^1O2,E}$) in sunlit surface water.

Antibiotics	H_2MLs^+	$HMLs^0$	MLs^-	$t_{1/2,E}$ (h) pH = 6.0 – 9.0
	$k_{\bullet OH,MLs} \times 10^{-9}$ (M^{-1} s^{-1})			$t_{\bullet OH,E}$
roxithromycin	1.09 ±0.30	2.38 ± 0.18	12.43 ± 3.20	86.98 – 175.50
clarithromycin	0.23 ± 0.01	2.83 ± 0.16	17.72 ± 0.02	76.88 – 787.49
spiramycin	3.70 ± 0.51	6.65 ± 0.35	104.25 ± 7.55	33.17 – 51.91
	$k_{^1O2,MLs} \times 10^{-7}$ (M^{-1} s^{-1})			$t_{^1O2,E}$
spiramycin	7.59 ± 0.84	11.65 ± 1.14	1154.29 ± 201.54	1.83 – 2.53

3.3. Phototransformation pathways

The UV-Vis photolytic intermediates of the three MLs in pure water were explored in order to reveal their main transformation pathways. The total ion chromatograms of the three compounds before and after photolysis, as well as the MS and MS^2 mass spectra in positive ionization mode areshown in Figs. S7 ~ S10, based on the chemical structures identified for eight photoproducts. Their corresponding retention times (t_R) and related fragment information are shown in Table S5.

The phototransformation pathways of the MLs are proposed according to their photoproducts (Fig. 3). As for ROX, the imine nitrogen (C=N−) on C substituent position was transformed to carbonyl groups (C=O), generating the corresponding product (P1, erythromycin, ERY) with fragment ions (e.g., *m*/*z* 576.5) matching those of ERY in the MS^2 spectra. This observation is in agreement with a previous study (Batchu et al. 2014). In addition, ROX was hydroxylated to P2 with a functional group of carboxyl, which peaked at retention time 11.461 min before the parent ROX. Thus, hydroxylation and carboxylation are likely to be the corresponding reactions. The phototransformation of CLA involves the following key pathways: stepwise hydroxylation

at the substituent groups −O−CH_3 to generate P3 and P4, and removal of methanol to form P5. For SPI, the main pathway is hydroxylated cleavage of carbon-oxygen-carbon bond (C−O−C), resulting in the formation of amino sugar parts (P6 and P7) and P8. This knowledge on the reaction pathways provides fundamental insights into the photochemical fate of MLs. Interestingly,, most of the intermediates retained the core backbone structures of the parent molecules, indicating that the toxicity or antibacterial activity might persist in these initial intermediates.

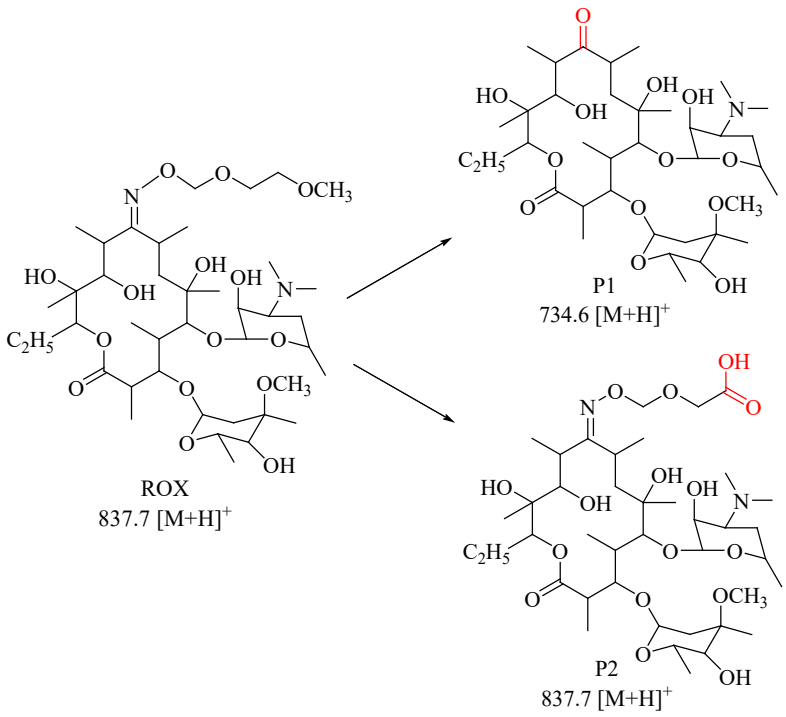

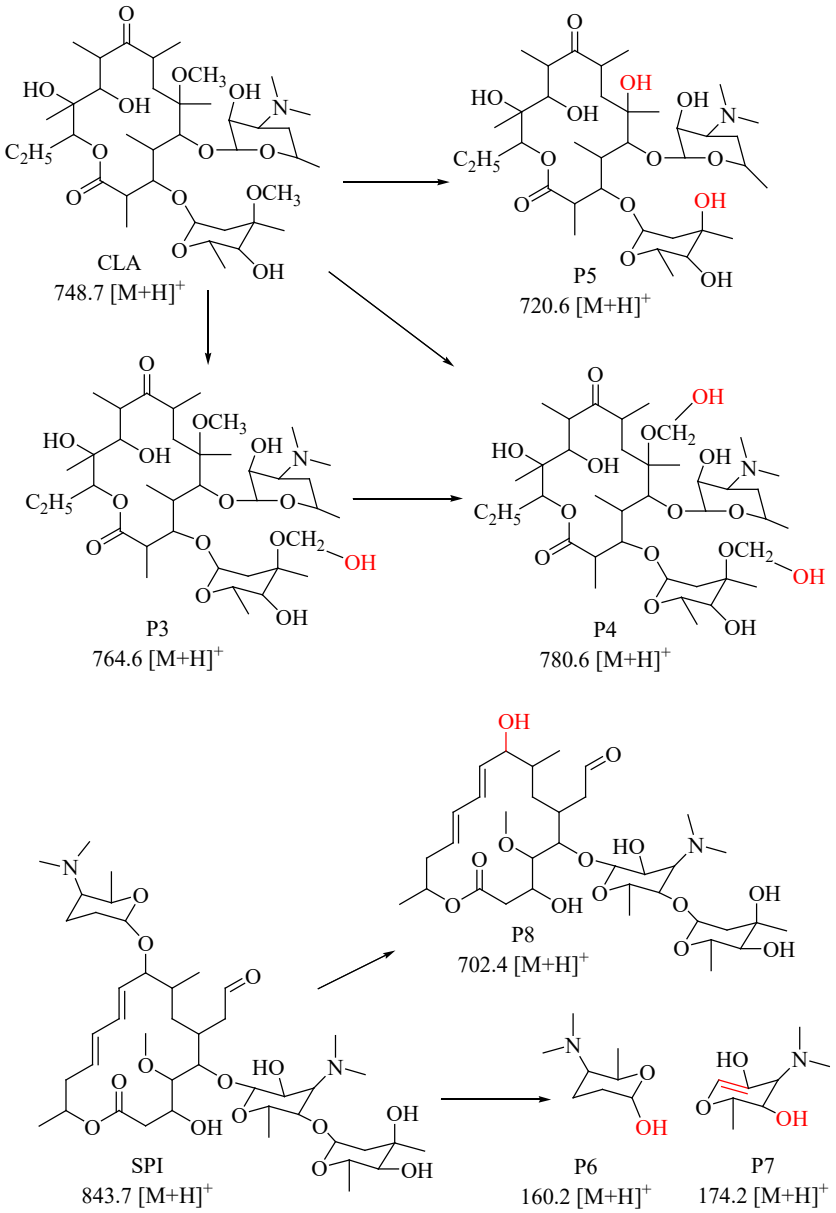

Fig. 3 Photodegradation products and pathways of the three MLs under UV-Vis irradiation

3.4 Photomodified toxicity to *Vibrio fischeri*

The toxicity of the three MLs during the irradiation was assessed, and the results are shown in Fig. 4. The luminescence inhibition rate (*I*%) of the parent MLs to *Vibrio fischeri* ranged from 35.38% for SPI to 37.64% for CLA. After irradiation, the three ML solutions exhibited a similar evolution of toxicity. During the photodegradation process, their toxicities initially increased, and subsequently decreased, and the maximum *I*% values of the photolyzed solutions

were significantly higher than those of the parent compounds ($p < 0.05$), implying the generation of more potent or toxic intermediates. Therefore, environment risk assessments should take into account the photochemical conversion of MLs.

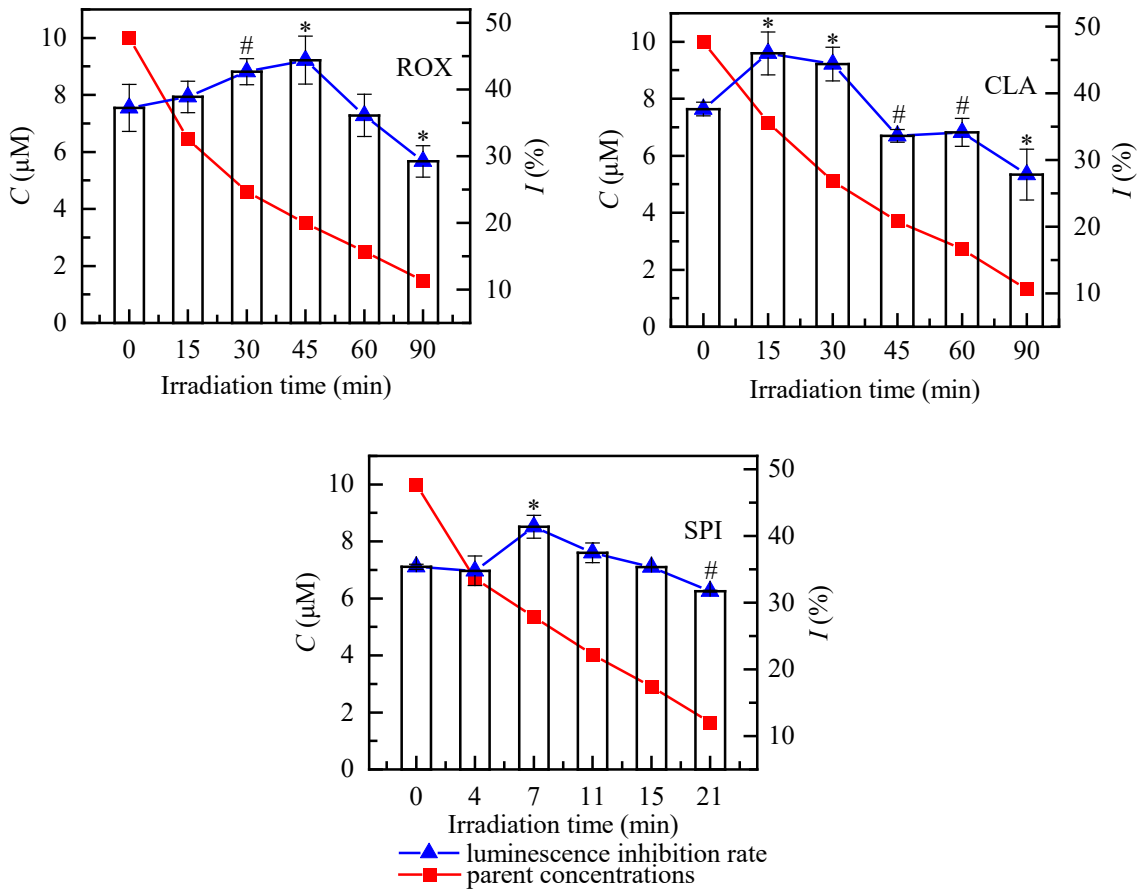

Fig. 4 Changes in concentrations (C) of photolyzed MLs, and luminescence inhibition rate (I%) of the photolyzed solutions to *Vibrio fischeri* with irradiation time

(The symbols * and # represent significant difference of the corresponding I% at the significance levels of 0.05 and 0.1, respectively, when compared to those values without irradiation)

4. Conclusion

This study comprehensively reports the aquatic photodegradation kinetics and fate of three ionizable macrolide antibiotics (ROX, CLA and SPI). Under simulated sunlight irradiation ($\lambda >$ 290 nm), CLA and SPI underwent significant photodegradation (compared to ROX), and followed pseudo-first-order kinetics. However, the three MLs were degraded rapidly under light that included shorter wavelengths (UV-Vis irradiation,$\lambda >$ 200 nm), and the k_p values were

found to be elevated with increasing pH. Among the dissociated forms, MLs^- photodegraded the fastest, followed by $HMLs^0$ and H_2MLs^+. The oxidation kinetics of MLs towards •OH and $^1O_2$ displayed pH dependence, which was attributable to the disparate reactivities of individual ML protonated species. The $k_{•OH,i}$ and $k_{^1O2,i}$ increased from H_2MLs^+ to $HMLs^0$ and MLs^-, and the MLs^- were the most highly reactive toward •OH and $^1O_2$. Moreover, the phototransformation pathways of MLs involved hydroxylation, carboxylation, and the cleavage of carbon-oxygen bond. The toxicities of photomodified MLs to *Vibrio fischeri* were significant which has implications for ecological risk assessments aimed at assessing and protecting aquatic habitats from antibiotic contamination. s. The photochemical behavior of MLs provided by this study provides a better understanding of the fate of these chemicals in engineered (e.g. wastewater treatment plants) and natural aquatic systems. .

Acknowledgements

This study was supported by the National Natural Science Foundation of China (21976045 and 22076112), and China Scholarship Council (CSC) Scholarship (202308610123, 202208610125). The authors are grateful to Guangkai He for the help in experiments.

Appendix A. Supplementary data

Supplementary data to this article can be found online at http://dx.doi.org/10.1016/j.w#########.

References

al Housari, F., Vione, D., Chiron, S., Barbati, S., 2010. Reactive photoinduced species in estuarine waters. Characterization of hydroxyl radical, singlet oxygen and dissolved organic matter triplet state in natural oxidation processes. Photochem. Photobiol. Sci. 9, 78-86.

Batchu, S.R., Panditi, V.R., O'Shea, K.E., Gardinali, P.R., 2014. Photodegradation of antibiotics under simulated solar radiation: Implications for their environmental fate. Sci. Total Environ. 470-471, 299-310.

Boreen, A.L., Arnold, W.A., McNeill, K., 2004. Photochemical fate of sulfa drugs in the aquatic

environment: Sulfa drugs containing five-membered heterocyclic groups. Environ. Sci. Technol. 38, 3933-3940.

Boreen, A.L., Arnold, W.A., McNeill, K., 2005. Triplet-sensitized photodegradation of sulfa drugs containing six-membered heterocyclic groups: Identification of an SO2 extrusion photoproduct. Environ. Sci. Technol. 39, 3630-3638.

Cooper, W.J., Zika, R.G., Petasne, R.G., Fischer, A.M. 1989, In: Suffet, I.H., MacCarthy, P. (Eds), Aquatic humic substances. American Chemical Society, Washington, DC, pp 333-362.

Edhlund, B.L., Arnold, W.A., McNeill, K., 2006. Aquatic photochemistry of nitrofuran antibiotics. Environ. Sci. Technol. 40, 5422-5427.

Garcia-Galan, M.J., Diaz-Cruz, M.S., Barcelo, D., 2012. Kinetic studies and characterization of photolytic products of sulfamethazine, sulfapyridine and their acetylated metabolites in water under simulated solar irradiation. Water Res. 46, 711-722.

Ge, L.K., Dong, Q.Q., Halsall, C., Chen, C.L., Li, J., Wang, D.G., Zhang, P., Yao, Z.W., 2018a. Aqueous multivariate phototransformation kinetics of dissociated tetracycline: Implications for the photochemical fate in surface waters. Environ. Sci. Pollut. Res. 25, 15726-15732.

Ge, L.K., Halsall, C., Chen, C.E., Zhang, P., Dong, Q.Q., Yao, Z.W., 2018b. Exploring the aquatic photodegradation of two ionisable fluoroquinolone antibiotics - Gatifloxacin and balofloxacin: Degradation kinetics, photobyproducts and risk to the aquatic environment. Sci. Total Environ. 633, 1192-1197.

Ge, L.K., Na, G.S., Chen, C.E., Li, J., Ju, M.W., Wang, Y., Li, K., Zhang, P., Yao, Z.W., 2016. Aqueous photochemical degradation of hydroxylated PAHs: Kinetics, pathways, and multivariate effects of main water constituents. Sci. Total Environ. 547, 166-172.

Ge, L.K., Na, G.S., Zhang, S.Y., Li, K., Zhang, P., Ren, H.L., Yao, Z.W., 2015. New insights into the aquatic photochemistry of fluoroquinolone antibiotics: Direct photodegradation, hydroxyl-radical oxidation, and antibacterial activity changes. Sci. Total Environ. 527-528, 12-17.

Ge, L.K., Yang, Y., Cao, S.K., Bai, D.X., Wei, X.X., Zhang, P., Ma, H.R., 2022. Aqueous environmental photochemical behavior of different antibiotic dissociation forms. Sci. China Chem. 52, 2183-2200.

Ge, L.K., Zhang, P., Halsall, C., Li, Y.Y., Chen, C.E., Li, J., Sun, H.L., Yao, Z.W., 2019. The

357 importance of reactive oxygen species on the aqueous phototransformation of sulfonamide
358 antibiotics: Kinetics, pathways, and comparisons with direct photolysis. Water Res. 149, 243-
359 250.
360 Geng, C., Liang, Z.J., Cui, F.Y., Zhao, Z.W., Yuan, C., Du, J.Y., Wang, C., 2020. Energy-saving
361 photo-degradation of three fluoroquinolone antibiotics under VUV/UV irradiation: Kinetics,
362 mechanism, and antibacterial activity reduction. Chem. Eng. J. 383, 123145.
363 Khajouei, G., Finklea, H.O., Lin, L.S., 2022. UV/chlorine advanced oxidation processes for
364 degradation of contaminants in water and wastewater: A comprehensive review. J. Environ.
365 Chem. Eng. 10, 107508.
366 Larson, R.A., Weber, E.J., 1996. Reaction mechanisms in environmental organic chemistry
367 Carbohydrate Polymers 29, 293-294.
368 Li, C.J., Zhang, D.H., Peng, J.L., Li, X.G., 2018. The effect of pH, nitrate, iron (III) and
369 bicarbonate on photodegradation of oxytetracycline in aqueous solution. J. Photochem.
370 Photobiol., A 356, 239-247.
371 Li, J., Li, W., Liu, K., Guo, Y., Ding, C., Han, J., Li, P., 2022. Global review of macrolide
372 antibiotics in the aquatic environment: Sources, occurrence, fate, ecotoxicity, and risk
373 assessment. J. Hazard. Mater. 439, 129628.
374 Li, S., Huang, T.B., Du, P.H., Liu, W., Hu, J.Y., 2020. Photocatalytic transformation fate and
375 toxicity of ciprofloxacin related to dissociation species: Experimental and theoretical
376 evidences. Water Res. 185, 116286.
377 Li, W., Xu, X.J., Lyu, B.L., Tang, Y., Zhang, Y.L., Chen, F., Korshin, G., 2019. Degradation of
378 typical macrolide antibiotic roxithromycin by hydroxyl radical: Kinetics, products, and
379 toxicity assessment. Environ. Sci. Pollut. Res. 26, 14570-14582.
380 LV, B.L., Li, W., Yu, X.L., Zhang, D., Zhang, Y.L., 2019. Effect of dissolved organic matter on
381 the photodegradation of roxithromycin. J. Environ. Sci. 39, 747-754.
382 Mill, T., 1999. Predicting photoreaction rates in surface waters. Chemosphere 38, 1379-1390.
383 Niu, J., Li, Y., Wang, W., 2013. Light-source-dependent role of nitrate and humic acid in
384 tetracycline photolysis: Kinetics and mechanism. Chemosphere 92, 1423-1429.
385 Schwarzenbach, R.P., Gschwend, P.M., Imboden, D.M., 2003. Environmental Organic
386 Chemistry (Second Edition). New Jersey: John Wiley & Sons, Inc.

Voigt, M., Jaeger, M., 2017. On the photodegradation of azithromycin, erythromycin and tylosin and their transformation products – A kinetic study. Sustain. Chem. Pharm. 5, 131-140.

Wei, X., Chen, J., Xie, Q., Zhang, S., Ge, L., Qiao, X., 2013. Distinct photolytic mechanisms and products for different dissociation species of ciprofloxacin. Environ. Sci. Technol. 47, 4284-4290.

Werner, J.J., Arnold, W.A., McNeill, K., 2006. Water hardness as a photochemical parameter: Tetracycline photolysis as a function of calcium concentration, magnesium concentration, and pH. Environ. Sci. Technol. 40, 7236-7241.

Willach, S., Lutze, H.V., Eckey, K., Loppenberg, K., Luling, M., Wolbert, J.B., Kujawinski, D.M., Jochmann, M.A., Karst, U., Schmidt, T.C., 2018. Direct Photolysis of Sulfamethoxazole Using Various Irradiation Sources and Wavelength Ranges-Insights from Degradation Product Analysis and Compound-Specific Stable Isotope Analysis. Environ. Sci. Technol. 52, 1225-1233.

Xie, Q., Chen, J.W., Zhao, H.X., Qiao, X.L., Cai, X.Y., Li, X.H., 2013. Different photolysis kinetics and photooxidation reactivities of neutral and anionic hydroxylated polybrominated diphenyl ethers. Chemosphere 90, 188-194.

Xu, H., Cooper, W.J., Jung, J.Y., Song, W.H., 2011. Photosensitized degradation of amoxicillin in natural organic matter isolate solutions. Water Res. 45, 632-638.

Yang, X., Xie, H., Chen, J., Li, X., 2013. Anionic phenolic compounds bind stronger with transthyretin than their neutral forms: Nonnegligible mechanisms in virtual screening of endocrine disrupting chemicals. Chem. Res. Toxicol. 26, 1340-1347.

Zhang, Z.C., Xie, X.D., Yu, Z.Q., Cheng, H.F., 2019. Influence of chemical speciation on photochemical transformation of three fluoroquinolones (FQs) in water: Kinetics, mechanism, and toxicity of photolysis products. Water Res. 148, 19-29.